

Characterization of Active Sites on Carbon Catalysts

José L. Figueiredo, Manuel F. R. Pereira, Maria M. A. Freitas, and José J. M. Órfão

A method based on the deconvolution of TPD spectra is proposed for the characterization of surface oxygen groups, which can act as the active sites on carbon catalysts. The method, which was previously used to characterize activated carbons oxidized in the gas phase, has been extended and applied to other materials, carbons oxidized in the liquid phase. It is shown that this method fits quite well the TPD experimental data of the original activated carbon as well as the gas-phase and liquid-phase oxidized materials and is suitable to estimate the amounts of each type of oxygen surface groups.

1. Introduction

Carbon materials are finding an increasing number of applications in catalysis, either as supports or as catalysts on their own. The success of these applications results from the specific properties of these materials, from the possibility of tailoring both their pore structure and their surface chemistry to meet the demands of the catalytic reaction envisaged.¹

The nature and concentration of functional groups on the surface of the carbon material is particularly relevant, as such groups can act as anchoring sites for the active phases, or their precursors, in the preparation of supported catalysts, or they can be the active sites for specific catalytic reactions. Oxygen functional groups are most important in this context, as they can be formed spontaneously by exposure to the atmosphere; in addition, the concentration of such groups can be further modified by oxidative and thermal treatments.²

Thus, it has been shown that homogeneous catalysts consisting of transition metal complexes can be anchored onto the surface of carbon materials by chemical bonding of functionalized ligands with oxygen functional groups on the carbon surface^{3,4} or by direct coordination of these to the metal center.⁵ Similar methodologies were used to prepare well-dispersed and stable carbon-supported metal catalysts, both by impregnation^{6–8} and by CVD.⁹

The same approach can be used to improve the performance of carbon-coated monoliths, a topic which is being developed by the group of Jacob Moulijn.^{10,11} Thus, in a recent report on the use of carbon-coated monoliths as supports for the immobilization of biocatalysts, it was shown that larger amounts of enzyme could be loaded upon an oxidation treatment, which increased the amounts of surface oxygen groups.¹² Clearly, the surface chemistry of the material must be modified according to the nature of the enzyme, to optimize such structured catalysts.

On the other hand, the decisive role of surface chemistry on the catalytic properties of carbon materials, which was recognized long ago,¹³ could only be quantitatively established recently, when suitable methods of analysis of the carbon surface groups became available. For instance, it has been shown that

carbonyl/quinone groups are the active sites for the oxidative dehydrogenation of ethylbenzene to styrene, and a linear correlation between the activity of carbon catalysts and the concentration of such sites was established.¹⁴ Similarly, the catalytic activity of carbon materials for the dehydration of methanol to dimethyl ether was correlated with the concentration of strong acid sites.¹⁵

Different techniques are available to characterize these materials, such as TPD, XPS, FTIR, and chemical or electrochemical titration methods.¹⁶ Nevertheless, none of these methods allows a straightforward quantitative analysis of the surface functional groups.

XPS is a surface technique that only gives an estimate of the chemical composition of the uppermost surface layers (about 10–15 nm in depth), which makes this technique ideal for surface analysis, for carbon fibers and graphites. When applied to porous carbons for the determination of the oxygen surface groups, XPS has the following drawbacks: (i) the external surface area is only a small fraction of the total surface area and it is not representative of all of the material; (ii) the holes in the surface can affect the final results because the surface is not flat; (iii) the analysis is made in high-vacuum, that is, under conditions quite different from those usually used in the applications of the carbon catalyst, and a rearrangement of the surface can occur; and (iv) deconvolution of the O1s and C1s peaks is not straightforward, and it is still a matter of discussion.

FTIR is mainly used as a qualitative technique for the evaluation of the chemical structure of carbon materials. It is not easy to get good spectra because carbons are black materials that absorb almost all of the radiation in the visible spectrum, and the peaks obtained are usually a sum of the interactions of different types of groups.¹⁷

Chemical analyses, such as the traditional Boehm titration method,¹⁸ present several drawbacks, such as: the equilibrium times are very long for microporous materials; there are problems of reproducibility when dealing with small amounts of sample; and this technique only can determine about 50% of the total oxygen available in activated carbons.¹⁹

TPD is a thermal analysis method that is becoming more popular for the characterization of the oxygen-containing groups of activated carbons. In this technique, all of the surface groups are thermally decomposed releasing CO and/or CO₂ and in some cases H₂O and H₂, at different temperatures. The nature of the groups can be assessed by the decomposition temperature and

Table 1. Textural Properties of Selected Materials

sample	V_{micro} $\text{cm}^3 \text{g}^{-1}$	S_{meso} $\text{m}^2 \text{g}^{-1}$	W_{01} $\text{cm}^3 \text{g}^{-1}$	W_{02} $\text{cm}^3 \text{g}^{-1}$	L nm
S	0.445	36	0.418	0.030	0.86
$\text{S}_{\text{O}_2,3\text{h}}$	0.447	69	0.395	0.075	1.2
$\text{S}_{\text{O}_2,10\text{h}}$	0.504	124	0.403	0.118	1.5
$\text{S}_{\text{N}_2\text{O},10\text{h}}$	0.508	28	0.494	0.096	1.2
$\text{S}_{\text{HNO}_3,6\text{h}}$	0.410	47	0.380	0.032	0.85

type of gas released, and their respective amounts by the areas of the peaks.² In this technique, all of the oxygen present is released and determined as CO, CO₂, and H₂O, as confirmed by comparing the oxygen obtained by TPD and by elemental analysis.² The major problem is the difficulty in identifying each surface group individually, because TPD spectra show composite CO and CO₂ peaks. In a previous work,² we presented a simplified method to deconvolute the TPD spectra to estimate the amount of each type of oxygen surface group for activated carbons oxidized in the gas phase. In this work, an extension of the previous method is proposed and applied not only to other gas-phase oxidized samples but also to liquid-phase oxidized materials. In our opinion, this method is suitable to estimate the type and amount of each surface group in a simple and easy way, and can be applied to all carbon catalysts.

2. Experimental Section

An activated carbon was prepared from a coconut shell char by activation with H₂O at 1173 K. It was subsequently oxidized in the gas phase, with 5% O₂ (in N₂) at 698 K or with 50% N₂O (in N₂) for different times, to achieve the desired burnoff (B.O.), and in the liquid phase, with 5 M nitric acid at the boiling temperature in a Soxhlet for different times. The materials oxidized in the liquid phase were subsequently washed with

distilled water until neutral pH, and dried in an oven at 383 K for 24 h. Thus, the following samples were prepared: S, original carbon; $\text{S}_{\text{O}_2,3\text{h}}$, S oxidized with 5% O₂ for 3 h at 698 K (B.O. = 12%); $\text{S}_{\text{O}_2,6\text{h}}$, S oxidized with 5% O₂ for 6 h at 698 K (B.O. = 19%); $\text{S}_{\text{O}_2,10\text{h}}$, S oxidized with 5% O₂ for 10 h at 698 K (B.O. = 42%); $\text{S}_{\text{N}_2\text{O},3\text{h}}$, S oxidized with 50% N₂O for 3 h at 773 K (B.O. = 5.3%); $\text{S}_{\text{N}_2\text{O},6\text{h}}$, S oxidized with 50% N₂O for 6 h at 773 K (B.O. = 14%); $\text{S}_{\text{N}_2\text{O},10\text{h}}$, S oxidized with 50% N₂O for 10 h at 773 K (B.O. = 30%); $\text{S}_{\text{HNO}_3,3\text{h}}$, S oxidized with 5 M nitric acid for 3 h at boiling temperature; and $\text{S}_{\text{HNO}_3,6\text{h}}$, S oxidized with 5 M nitric acid for 6 h at boiling temperature.

The textural characterization of the materials was based on the N₂ adsorption isotherms, determined at 77 K with a Coulter Omnisorp 100 CX apparatus. BET surface areas were calculated, as well as the micropore volumes (V_{micro}) and mesopore surface areas (S_{meso}) according to the *t*-method. The adsorption data were also analyzed with the Dubinin equation. When a type IV deviation occurred, two microporous structures were taken into account, and the corresponding volumes, W_{01} and W_{02} , were calculated. The Stoekli equation was used to estimate the average micropore width of the smaller pores (L).

The TPD profiles were obtained with a custom built setup, consisting of a U-shaped tubular microreactor, placed inside an electrical furnace. The mass flow rate of the helium carrier gas (69 $\mu\text{g/s}$) and the heating rate of the furnace (5 K/min) were controlled with appropriate units. The amounts of CO and CO₂ desorbed from the carbon samples (0.1 g) were monitored with a SPECTRAMASS Dataquad quadrupole mass spectrometer.

3. Results and Discussion

3.1. Textural Characterization. Table 1 shows the textural properties of selected samples. It may be observed that gas-

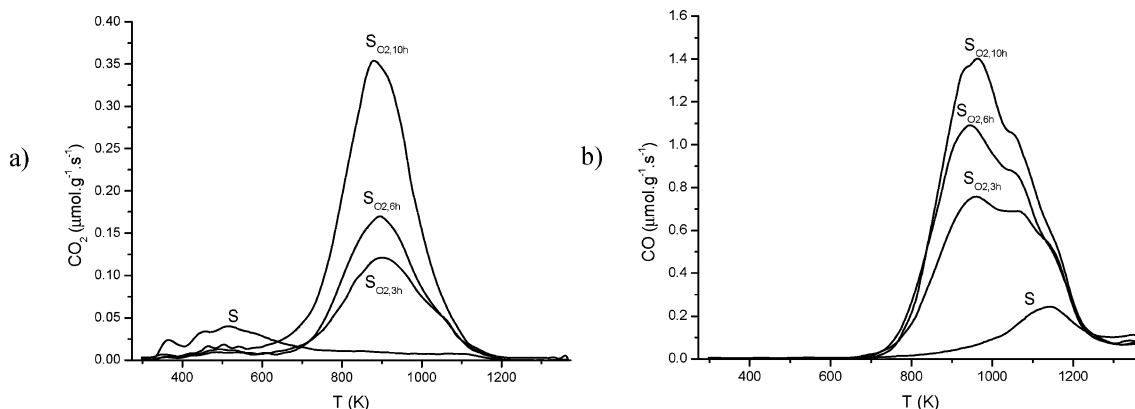


Figure 1. TPD spectra for the samples oxidized in 5% O₂ in N₂: (a) CO₂ evolution; (b) CO evolution.

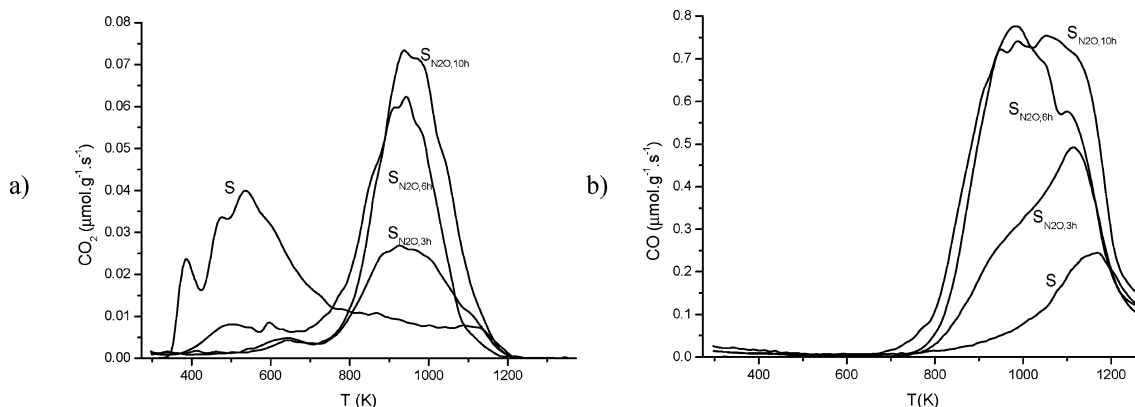


Figure 2. TPD spectra for the samples oxidized in 50% N₂O in N₂: (a) CO₂ evolution; (b) CO evolution.

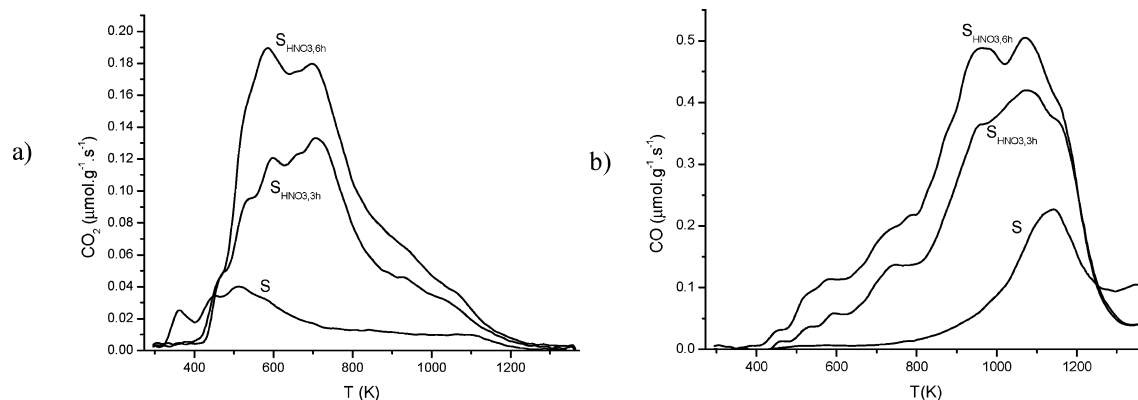


Figure 3. TPD spectra for the samples oxidized with HNO₃ 5 M: (a) CO₂ evolution; (b) CO evolution.

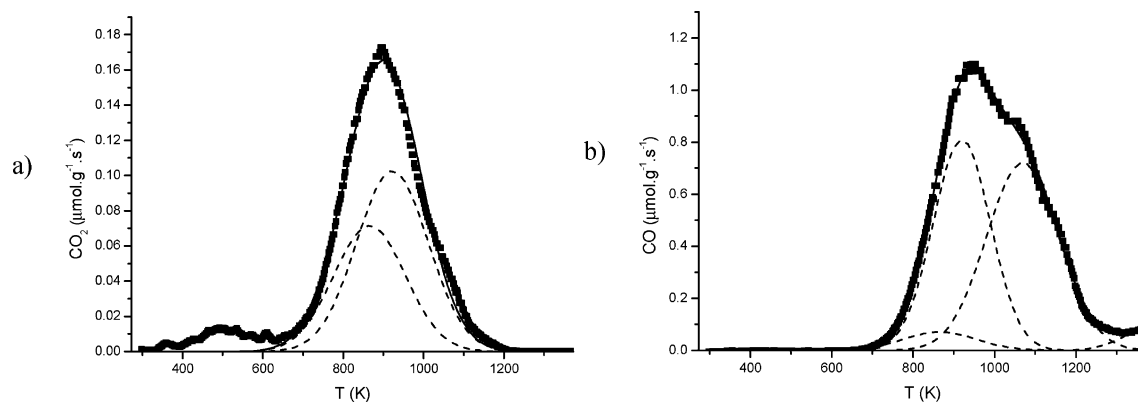


Figure 4. Deconvolution of TPD spectra for the sample S_{O₂,6h}: (a) CO₂ spectrum; (b) CO spectrum (■, TPD experimental data; ---, individual peaks; —, sum of the individual peaks).

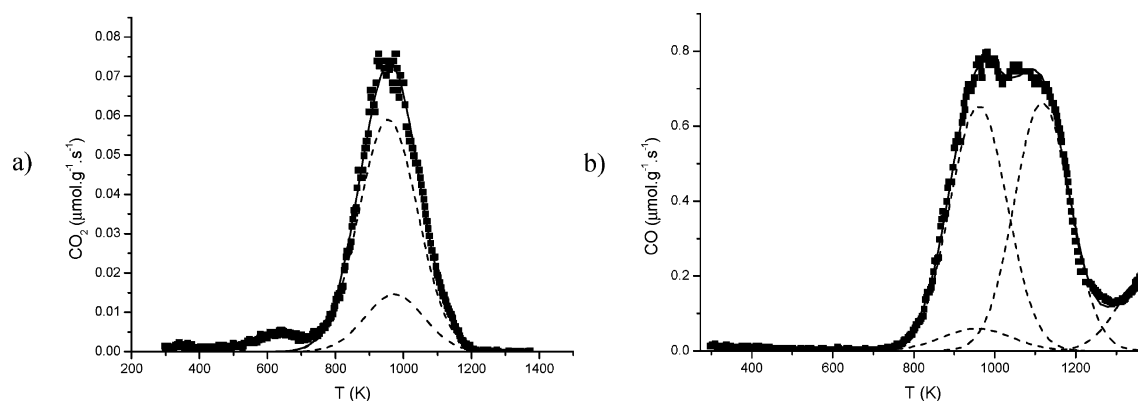


Figure 5. Deconvolution of TPD spectra for the sample S_{N₂O,10h}: (a) CO₂ spectrum; (b) CO spectrum (■, TPD experimental data; ---, individual peaks; —, sum of the individual peaks).

phase oxidations increase the micropore volume, the mesopore surface area, and the average micropore width (S_{O₂,3h}, S_{O₂,6h}, and S_{O₂,10h} vs S), with the exception of the N₂O oxidation that slightly decreases the mesopore surface area. Liquid-phase oxidation has no significant impact on the textural properties (S_{HNO₃,6h} vs S).

3.2. Surface Chemistry Characterization. The surface chemistry was evaluated using different techniques: elemental analysis, FTIR, XPS, chemical titrations (Boehm's method), and TPD. The results of the first four techniques are not shown here, but in all cases an increase in the oxygen content with the extent of the oxidation treatment was observed. In this work, only TPD results are analyzed in detail. Figures 1–3 show the TPD results for the oxidized samples considered in this work. It can be observed that gas-phase oxidations (Figures 1 and 2) increase mainly the CO releasing groups at around 950 K (phenol groups) and 1100 K (carbonyl/quinone groups) and CO₂ releasing groups

at around 850 K (carboxyl anhydride groups) and 950 K (lactone groups). In these samples, no carboxylic acid groups are present, because they decompose at temperatures below those used for the oxidation. Liquid-phase treatments (Figure 3) have the particularity to increase the carboxylic groups, which are released as CO₂ at low temperatures (below 800 K).

3.3. Deconvolution of TPD Spectra. To determine the amount of each surface group, the deconvolution of the CO and CO₂ TPD spectra was carried out. A multiple Gaussian function was used for fitting each of the TPD spectra, taking the position of the peak center as the initial estimate. The numerical calculations were based on a nonlinear routine, which minimized the square of the deviations, using the Levenberg–Marquardt method to perform the iterations. The use of Gaussian functions is justified by the shape of the TPD peaks, which are a result of a continuous random distribution of binding energies

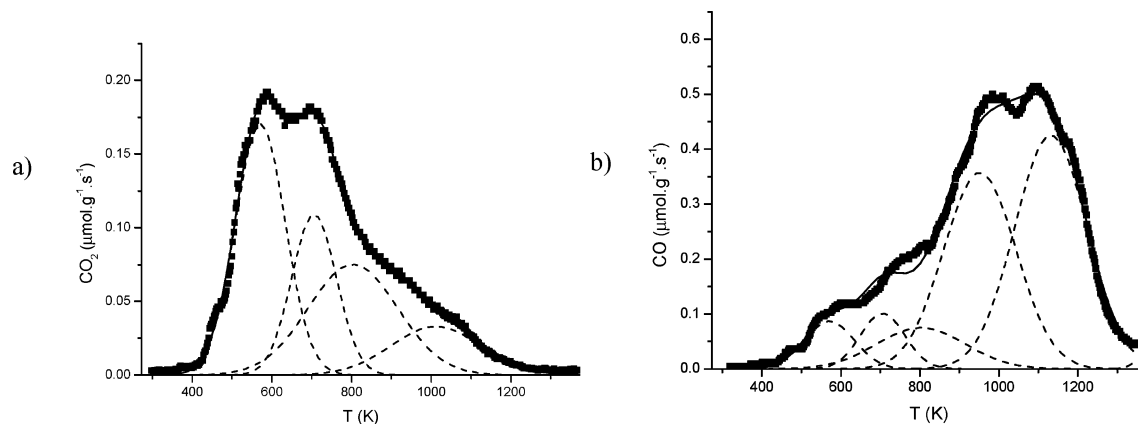


Figure 6. Deconvolution of TPD spectra for the sample $\text{SHNO}_{3,6\text{h}}$: (a) CO_2 spectrum; (b) CO spectrum (■, TPD experimental data; ---, individual peaks; —, sum of the individual peaks).

Table 2. Results of the Deconvolution of CO_2 TPD Spectra Using a Multiple Gaussian Function

sample	peak #1			peak #2			peak #3			peak #4		
	T_M (K)	W (K)	A ($\mu\text{mol g}^{-1}$)	T_M (K)	W (K)	A ($\mu\text{mol g}^{-1}$)	T_M (K)	W (K)	A ($\mu\text{mol g}^{-1}$)	T_M (K)	W (K)	A ($\mu\text{mol g}^{-1}$)
S	511	157	81.2	650	206	54.7	884	173	28.9	1095	173	23.9
$\text{SO}_{2,3\text{h}}$							885	209	107	917	209	268
$\text{SO}_{2,6\text{h}}$							886	178	192	922	178	275
$\text{SO}_{2,10\text{h}}$							876	174	540	904	174	373
$\text{SN}_2\text{O}_{,3\text{h}}$							940	219	73.2	970	219	16.8
$\text{SN}_2\text{O}_{,6\text{h}}$							919	168	128	975	168	32.4
$\text{SN}_2\text{O}_{,10\text{h}}$							955	172	152	973	172	374
$\text{SHNO}_{3,3\text{h}}$	571	149	228	716	123	166	822	228	131	1005	228	86.5
$\text{SHNO}_{3,6\text{h}}$	571	125	322	706	112	184	803	224	253	1012	224	111

Table 3. Results of the Deconvolution of CO TPD Spectra Using a Multiple Gaussian Function

sample	peak #1			peak #2			peak #3			peak #4			peak #5		
	T_M (K)	W (K)	A ($\mu\text{mol g}^{-1}$)	T_M (K)	W (K)	A ($\mu\text{mol g}^{-1}$)	T_M (K)	W (K)	A ($\mu\text{mol g}^{-1}$)	T_M (K)	W (K)	A ($\mu\text{mol g}^{-1}$)	T_M (K)	W (K)	A ($\mu\text{mol g}^{-1}$)
S	511	157	0.4	650	206	22.0	884	173	28.9	998	146	103	1158	146	474
$\text{SO}_{2,3\text{h}}$							885	209	107	939	154	1548	1105	154	1272
$\text{SO}_{2,6\text{h}}$							886	178	192	933	154	2184	1091	154	1452
$\text{SO}_{2,10\text{h}}$							876	174	540	947	140	2484	1094	140	1500
$\text{SN}_2\text{O}_{,3\text{h}}$							940	219	73.2	957	138	470	1116	138	940
$\text{SN}_2\text{O}_{,6\text{h}}$							919	168	128	945	156	1356	1096	156	1178
$\text{SN}_2\text{O}_{,10\text{h}}$							955	172	152	959	138	1356	1116	138	1392
$\text{SHNO}_{3,3\text{h}}$	571	149	73.2	716	123	157	822	228	131	957	172	780	1128	172	892
$\text{SHNO}_{3,6\text{h}}$	571	125	164	706	112	170	803	224	253	952	183	985	1132	183	1172

of the surface groups.²⁰ For the gas-phase oxidized samples, the assumptions made and justified in a previous work² were followed:

(a) The CO_2 spectra are decomposed into two contributions, corresponding to carboxylic anhydrides (CO_2 peak #3) and lactones (CO_2 peak #4). There is not any low-temperature CO_2 evolution, because these samples were processed at a temperature higher than the decomposition of carboxylic acids.

(b) The carboxylic anhydrides decompose by releasing one CO and one CO_2 molecule. Thus, for samples oxidized in the gas phase, the first component in the CO spectrum corresponds to the carboxylic anhydrides, with a peak of the same shape as and equal magnitude to the CO_2 peak #3 (CO peak #3). This peak is pre-defined from the deconvolution of the CO_2 spectra.

(c) In addition to the carboxylic anhydrides (CO peak #3), the CO spectrum includes contributions from phenols (CO peak #4) and carbonyl/quinones (CO peak #5).

(d) It is assumed that secondary reactions at high temperatures are negligible.

(e) In the CO_2 spectrum, the width at half-height was taken the same for both peaks.

Two additional assumptions were made in the present work:

(f) A new CO peak around 1370 K was included (CO peak #6). This results from the observation that the CO spectrum does not return to the baseline at high temperatures, and it seems that a new peak is being formed at those temperatures. This peak can be assigned to basic groups, such as pyrones and chromenes,²¹ or may result from the rearrangement of the surface because temperatures are higher than those used in the preparation of these samples. This peak was used for the deconvolution, but it was not taken into consideration for quantitative analysis.

(g) The same width at half-height was considered for the phenol and carbonyl groups. This was necessary mainly in the case of samples where there were no peak shoulders.

To use this method to fit also the TPD spectra of activated carbons oxidized in the liquid phase, the following assumptions were necessary:

(h) There are two types of carboxylic groups, which can be assigned to strongly acidic (CO_2 peak #1) and less acidic (CO_2 peak #2) carboxylic groups.²¹

(i) The CO spectra of these samples present shoulders at low temperatures that cannot be justified by the carboxylic anhydride groups. These shoulders appear in the same region of the decomposition of the carboxylic groups. In the literature, it is

always assumed that these groups decompose releasing only CO₂. Our results show that some CO is formed at the same time. The release of CO at similar temperatures can be observed in the literature for several TPD's spectra from HNO₃ oxidized carbons.^{22–24} A possible justification could be related to the fact that when CO₂ molecules are released in the micropores, they are always in the proximity of the surfaces, and thus there is a high probability of interaction with unoccupied active sites just formed by the decomposition of other carboxylic groups originating another surface complex (C[O]) and a free CO.²⁵ To verify the validity of this explanation, two additional TPD experiments were carried out. In the first one, the TPD experiment was stopped at 573 K, and several CO₂ pulses were introduced at this temperature. There was no CO formation, meaning that the previous justification does not apply to the present situation. In addition, the TPD at high temperatures of the sample previously submitted to the CO₂ pulses is coincident with the TPD of the original sample, showing that no new oxygen surface groups releasing CO at high temperatures were formed. In the second experiment, a flow of CO₂ was introduced at 573 K during 1 h in a sample previously submitted to a thermal treatment up to 1373 K in He flow (the equivalent of a TPD experiment). Afterward, a new TPD of this sample was carried out, which showed a TPD profile coincident with the original sample previously treated at 1373 K. This result shows that no oxygen surface groups are introduced when CO₂ contact with an activated carbon sample at 573 K. These two experiments show that CO is not released as a secondary reaction when the carboxylic acid groups are decomposed releasing CO₂. Nevertheless, as it was observed experimentally that these small CO peaks at low temperatures are released at the same time as the CO₂ peaks, it was assumed that for activated carbons oxidized in the liquid phase there are two CO peaks at low temperature (CO peaks #1 and #2) with the same peak center and width at half-height of those obtained for the carboxylic groups in the CO₂ peak. Almost all of the authors ignore the CO peaks at low temperature, but according to Moreno-Castilla et al.,²⁶ based on the work of Surygala et al.,²⁷ the CO peak that appears at low temperatures probably comes from the decomposition of carbonyl groups in α -substituted ketones and aldehydes.

Figures 4–6 show examples of the deconvolutions obtained with the activated carbons oxidized with O₂, N₂O, and HNO₃, respectively, which fit the data quite well, both for CO and for CO₂.

Tables 2 and 3 show the results obtained, where T_M is the temperature of the peak maximum, W is the width of the peak at half-height, and A is the integrated peak area. It can be observed that all of the fits give approximately the same values of T_M and W for each component, when applied to the original activated carbon or to the modified carbons containing quite different types and amounts of surface groups.

Thus, the peak maxima found were between 510 and 570 K for the strongly acidic carboxylic groups, 650 and 720 K for the less acidic carboxylic groups, 800 and 900 K for anhydrides, 900 and 1000 K for lactones, 940 and 990 K for phenols, and 1090 and 1150 K for carbonyls/quinones.

4. Conclusions

In this work, a series of activated carbons with different surface chemistries was prepared and characterized. A new method to deconvolute the TPD spectra, using multiple Gaussian functions, was applied to estimate the amount of each type of oxygen surface group. This method proved to fit quite well the

experimental data of nontreated, gas-phase oxidized and liquid-phase oxidized activated carbons, with different types and amounts of each oxygen surface group. This deconvolution method is easy to use and can be applied to characterize the active sites of carbon catalysts.

Acknowledgment

This work was carried out with support from Fundação para a Ciência e a Tecnologia (FCT, Portugal) and POCI 2010, with coparticipation from FEDER, Project POCI/EQU/57369/2004 “Nanostructured carbon catalysts”. Laboratório de Catálise e Materiais (LCM) is a research unit of Laboratório Associado LSRE-LCM.

Literature Cited

- (1) Rodríguez-Reinoso, F. The role of carbon materials in heterogeneous catalysis. *Carbon* **1998**, *36*, 159–175.
- (2) Figueiredo, J. L.; Pereira, M. F. R.; Freitas, M. M. A.; Órfão, J. J. M. Modification of the surface chemistry of activated carbons. *Carbon* **1999**, *37*, 1379–1389.
- (3) Silva, A. R.; Vital, J.; Figueiredo, J. L.; Freire, C.; de Castro, B. Activated carbons with immobilised manganese(III) salen complexes as heterogeneous catalysts in the epoxidation of olefins: influence of support and ligand functionalisation on selectivity and reusability. *New J. Chem.* **2003**, *27*, 1511–1517.
- (4) Silva, A. R.; Martins, M.; Freitas, M. M. A.; Figueiredo, J. L.; Freire, C.; de Castro, B. Anchoring of copper(II) acetylacetonate onto an activated carbon functionalised with a triamine. *Eur. J. Inorg. Chem.* **2004**, 2027–2035.
- (5) Silva, A. R.; Budarin, V.; Clark, J. H.; de Castro, B.; Freire, C. Chiral manganese(III) Schiff base complexes anchored onto activated carbon as enantio selective heterogeneous catalysts for alkene epoxidation. *Carbon* **2005**, *43*, 2096–2105.
- (6) Aksoylu, A. E.; Madalena, M.; Freitas, A.; Pereira, M. F. R.; Figueiredo, J. L. The effects of different activated carbon supports and support modifications on the properties of Pt/AC catalysts. *Carbon* **2001**, *39*, 175–185.
- (7) Fraga, M. A.; Jordão, E.; Mendes, M. J.; Freitas, M. M. A.; Faria, J. L.; Figueiredo, J. L. Properties of carbon-supported platinum catalysts: Role of carbon surface sites. *J. Catal.* **2002**, *209*, 355–364.
- (8) Job, N.; Pereira, M. F. R.; Lambert, S.; Cabiac, A.; Delahay, G.; Colomer, J. F.; Marien, J.; Figueiredo, J. L.; Pirard, J. P. Highly dispersed platinum catalysts prepared by impregnation of texture-tailored carbon xerogels. *J. Catal.* **2006**, *240*, 160–171.
- (9) Aksoylu, A. E.; Faria, J. L.; Pereira, M. F. R.; Figueiredo, J. L.; Serp, P.; Hierso, J. C.; Feurer, R.; Kihn, Y.; Kalck, P. Highly dispersed activated carbon supported platinum catalysts prepared by OMCVD: a comparison with wet impregnated catalysts. *Appl. Catal., A* **2003**, *243*, 357–365.
- (10) Vergunst, T.; Linders, M. J. G.; Kapteijn, F.; Moulijn, J. A. Carbon-based monolithic structures. *Catal. Rev.* **2001**, *43*, 291–314.
- (11) Crezee, E.; Barendregt, A.; Kapteijn, F.; Moulijn, J. A. Carbon coated monolithic catalysts in the selective oxidation of cyclohexanone. *Catal. Today* **2001**, *69*, 283–290.
- (12) De Lathouder, K. M.; Lozano-Castelló, D.; Linares-Solano, A.; Kapteijn, F.; Moulijn, J. A. Carbon coated monoliths as support material for a lactase from *Aspergillus oryzae*: Characterization and design of the carbon carriers. *Carbon* **2006**, *44*, 3053–3063.
- (13) Weiss, D. The catalytic properties of amorphous carbon. *Proc. 5th Conf. Carbon*; 1962; Vol. 1, pp 65–72.
- (14) Pereira, M. F. R.; Órfão, J. J. M.; Figueiredo, J. L. Oxidative dehydrogenation of ethylbenzene on activated carbon catalysts. I. Influence of surface chemical groups. *Appl. Catal., A* **1999**, *184*, 153–160.
- (15) Moreno-Castilla, C.; Carrasco-Marin, F.; Parejo-Perez, C.; Ramon, M. V. L. Dehydration of methanol to dimethyl ether catalyzed by oxidized activated carbons with varying surface acidic character. *Carbon* **2001**, *39*, 869–875.
- (16) Leon y Leon, C.; Radovic, L. R. Interfacial chemistry and electrochemistry of carbon surfaces. In *Chemistry and Physics of Carbon*; Thrower, P. A., Ed.; Marcel Dekker: New York, 1994; Vol. 24, pp 213–310.
- (17) Zawadzki, J. Infrared spectroscopy in surface chemistry of carbons. In *Chemistry and Physics of Carbon*; Thrower, P. A., Ed.; Marcel Dekker: New York, 1988; Vol. 21, pp 147–386.

- (18) Boehm, H. P. Surface oxides on carbon and their analysis: a critical assessment. *Carbon* **2002**, 40, 145–149.
- (19) Boehm, H. P. Surface oxides on carbon. *High Temp.-High Pressures* **1990**, 22, 275–288.
- (20) Calo, J. M.; Hall, P. J. Applications of energetic distributions of oxygen surface complexes to carbon and char reactivity and characterization. In *Fundamental Issues in the Control of Carbon Gasification Reactivity*; Lahaye, J., Ehrburger, P., Eds.; Kluwer Academic Publishers: Dordrecht, The Netherlands, 1991; pp 329–368.
- (21) Zielke, U.; Huttinger, K. J.; Hoffman, W. P. Surface-oxidized carbon fibers. 1. Surface structure and chemistry. *Carbon* **1996**, 34, 983–998.
- (22) Otake, Y.; Jenkins, R. G. Characterization of oxygen-containing surface complexes created on a microporous carbon by air and nitric-acid treatment. *Carbon* **1993**, 31, 109–121.
- (23) Vinke, P.; Vandereijk, M.; Verbree, M.; Voskamp, A. F.; Vanbekum, H. Modification of the surfaces of a gas-activated carbon and a chemically activated carbon with nitric-acid, hypochlorite, and ammonia. *Carbon* **1994**, 32, 675–686.
- (24) Haydar, S.; Moreno-Castilla, C.; Ferro-Garcia, M. A.; Carrasco-Marin, F.; Rivera-Utrilla, J.; Perrard, A.; Joly, J. P. Regularities in the temperature-programmed desorption spectra of CO₂ and CO from activated carbons. *Carbon* **2000**, 38, 1297–1308.
- (25) Hall, P. J.; Calo, J. M.; Lilly, W. D. The energetic heterogeneity of coal char surfaces: effects of heating rate on TPD spectra. In *Proceedings of the International Conference on Carbon, Carbon' 88*; McEnaney, B., Mays, T. J., Eds.; IOP Publishing Co.: Bristol, U.K., 1988; pp 77–79.
- (26) Moreno-Castilla, C.; Carrasco-Marin, F.; Mueden, A. The creation of acid carbon surfaces by treatment with (NH₄)₂S₂O₈. *Carbon* **1997**, 35, 1619–1626.
- (27) Surygala, J.; Wandas, R.; Sliwka, E. Oxygen elimination in the process of noncatalytic liquefaction of brown coal. *Fuel* **1993**, 72, 409–411.